Bull. Soc. R. Sci. Liège, 2024, **93**(2), 560–571 *Peer-reviewed conference paper*
doi:10.25518/0037-9565.11795

Initial Results of our Spectro-photometric Monitoring of XZ Tau

Arpan GHOSH[1,#,*], Saurabh SHARMA[1], Joe Philip NINAN[2], Devendra Kumar OJHA[2], Aayushi VERMA[1], Tarak Chand SAHU[1], Rakesh PANDEY[3] and Koshvendra SINGH[2]

[1] Aryabhatta Research Institute of Observational Sciences (ARIES), Manora Peak, Nainital–263 001, India
[2] Department of Astronomy and Astrophysics, Tata Institute of Fundamental Research (TIFR), Mumbai–400 005, Maharashtra, India
[3] Physical Research Laboratory, Navrangpura, Ahmedabad–380 009, India
[#] Now at: Instituto de Radioastronomía y Astrofísica, Universidad Nacional Autónoma de México, Antigua Carretera a Pátzcuaro 8701, Ex-Hda San José de la Huerta, Morelia 58089, Michoacán, México
[*] Corresponding author: 19aghosh91@gmail.com

Paper presented at the 3rd BINA Workshop on "Scientific Potential of the Indo-Belgian Cooperation", held at the Graphic Era Hill University, Bhimtal (India), 22nd–24th March 2023.

Abstract

We present here initial results of our spectro-photometric monitoring of XZ Tau. During our monitoring period, XZ Tau exhibited several episodes of brightness variations in timescales of months at optical wavelengths in contrast to the mid-infrared wavelengths. The color evolution of XZ Tau during this period suggests that the brightness variations are driven by changes in accretion from the disc. The mid-infrared light curve shows an overall decline in brightness by ~ 0.5 and 0.7 magnitudes respectively in WISE $W1$ (3.4 μm) and $W2$ (4.6 μm) bands. The emission profile of the hydrogen recombination lines along with that of Ca II IRT lines points towards magnetospheric accretion of XZ Tau. We have detected P Cygni profile in Hβ indicating of out-flowing winds from regions close to accretion. Forbidden transitions of oxygen are also detected, likely indicating jets originating around the central pre-main sequence star.

Keywords: Star formation, Young Stellar Object, Eruptive variables, Episodic Accretion

1. Introduction

The process of accretion is fundamental in the formation of stars even though it is poorly understood (Hartmann et al., 2016). Initially, a steady state accretion rate was theorized for the formation of stars (Larson, 1969; Shu, 1977; Terebey et al., 1984). However, the observed discrepancy in the luminosity of Class I young stellar objects (YSOs) with that of the theoretical models gave rise to the 'Luminosity Problem' (Kenyon et al., 1990; Evans et al., 2009). The idea of 'episodic accretion' at early stages of pre-main sequence (PMS) evolution came up as a possible solution to the luminosity problem. Observations indicate that episodic accretion

phenomena span the entire PMS evolutionary stages from Class 0 to Class II (Safron et al., 2015). Various theoretical models have been proposed to explain the origin of the circumstellar disk instabilities that lead to the episodic outbursts. These models range from gravitational instabilities to external perturbations by an eccentric binary (Audard et al., 2014).

The phenomenon of episodic accretion was first observed in 1936 when FU Ori underwent an outburst of > 5 magnitudes in the V band. Since then, around 33 sources have been discovered that have demonstrated episodic accretion behavior with outburst magnitudes > 2 magnitudes in the V band, along with a wide variety of rise and decay timescales (Audard et al., 2014). YSOs that exhibit episodic accretion behavior are classified as FUors and EXors using a binary classification approach. FUor outbursts are manifested as 4–5 magnitude variations in the V band with absorption features in their spectrum and outburst timescales of decades. EXors on the other hand, undergo outbursts of 2–3 magnitudes with their spectra consisting of emission features and outburst timescales of 1–2 years.

In this paper, we will be presenting initial results of our spectro-photometric monitoring of a YSO, XZ Tau. Lorenzetti et al. (2009) classified XZ Tau as a bonafide EXor. It is located at an approximate distance of 140 pc in the L1551 dark cloud of Taurus star-forming region. Previously, Lorenzetti et al. (2012) and Audard et al. (2014) have reported irregular brightness variations in optical wavelengths with timescales of months. They have attributed these variations to short scale enhancements of disk accretion. However, simultaneous multi-wavelength photometric monitoring backed with spectroscopic observations is lacking. Such studies will enable us to understand the origin of such small scale enhancements in accretion rate, thus motivating us to carry out the monitoring of XZ Tau. This paper is arranged as follows: Section 2 describes the observations and the data reduction techniques employed. In Sect. 3, we describe the photometric and spectroscopic evolution of XZ Tau during our monitoring period and finally in Sect. 4 we conclude this paper based on our findings in Sect. 3.

2. Observation and Data Reduction

2.1. Photometric data

We have obtained multi-epoch photometric data of XZ Tau in broadband optical and mid-infrared (MIR) filters. The optical monitoring was obtained using the archival data from the Palomar Transient Factory (PTF; for details, see Law et al., 2009), the Asteroid Terrestrial-impact Last Alert System (ATLAS; for details, see Tonry et al., 2018), the Zwicky Transient Facility (ZTF; for details, see Bellm et al., 2019), and the American Association for the Variable Star Observers (AAVSO). The optical data was obtained in Johnson–Cousins (AAVSO observations are in the Johnson-Cousins filter system) B (0.44 μm), V (0.55 μm), R (0.65 μm) and I (0.80 μm), PTF g (0.477 μm) and R (0.63 μm), ZTF zg (0.48 μm) and zr (0.64 μm) and ATLAS *cyan* (0.53 μm) and *orange* (0.68 μm) bands. Time series MIR data were obtained from the Near-Earth Object Wide-field Infrared Survey Explorer (NEOWISE) survey (for details, see Mainzer et al., 2014). The MIR observations are in $W1$ (3.4 μm) and $W2$ (4.6 μm) bands and are obtained from the NASA/IPAC Infrared Science archive (https://irsa.ipac.caltech.edu/Missions/wise.html).

Table 1: Log of spectroscopic observations.

Telescope	Date	Grism	Wavelength Range	Resolution R	Exposure Time
3.6 m DOT (TANSPEC)	23/20/2020	Cross-dispersed	0.55–2.5 μm	$\sim$ 1500	120 s $\times$ 4 frames
2 m HCT (HFOSC)	22/02/2023	Gr7	0.38–0.68 μm	$\sim$ 1200	1500 s
2 m HCT (HFOSC)	22/02/2023	Gr8	0.58–0.84 μm	$\sim$ 2000	1500 s

2.2. Spectroscopic data

We have spectroscopically monitored XZ Tau during two epochs using the Hanle Faint Object Spectrograph Camera (HFOSC) of the 2 m Himalayan *Chandra* Telescope (HCT) – details about the HFOSC instrument are available at https://www.iiap.res.in/iao/hfosc.html – and the TIFR–ARIES Near-infrared Spectrometer (TANSPEC) of the 3.6 m Devasthal Optical Telescope (DOT; Sharma et al., 2022). Table 1 contains the log of spectroscopic observations.

The HFOSC observations were obtained using grisms Gr. 7 and Gr. 8 which provide a resolution of $R \sim 2000$ providing wavelength coverage of 0.4 to 0.9 μm. The HFOSC spectrum was reduced and calibrated using the standard IRAF modules. IRAF is distributed by National Optical Astronomy Observatories, USA, which is operated by the Association of Universities for Research in Astronomy, Inc., under cooperative agreement with the National Science Foundation for performing image processing. The details of the reduction and calibration procedures are described in detail in Ghosh et al. (2023a). TANSPEC observations were obtained using 1$''$ slit that provides a resolution of $R \sim 1500$ providing a wavelength coverage of 0.55 to 2.5 μm. The TANSPEC spectrum is reduced using the TANSPEC data reduction pipeline named pyTANSPEC (Ghosh et al., 2023b). Other details of the TANSPEC data reduction procedure have been outlined in Ghosh et al. (2023a).

3. Results and Analysis

3.1. Light curve

Figure 1 shows the light curve (LC) of XZ Tau spanning an almost ten year period, beginning from 2013 to 2023. The typical uncertainties in the optical bands is below 0.05 magnitudes. During this period, XZ Tau has exhibited multiple episodes of brightness variations in optical bands. XZ Tau brightened by about 1.3, 1.1, 0.9, and 0.8 magnitudes in optical B, V, R, and I bands respectively between March 28, 2013 and March 03, 2014. We do not have photometric coverage in the subsequent months of 2014; however, we see another episode of 1 magnitude brightening in the V band between November 09, 2014 and February 21, 2015. Next we observe that XZ Tau displays a peak brightness of 11.5 magnitudes in the *orange* band on September 03, 2017 and is gradually decaying to 12.6 magnitude on December 26, 2017. It started to brighten

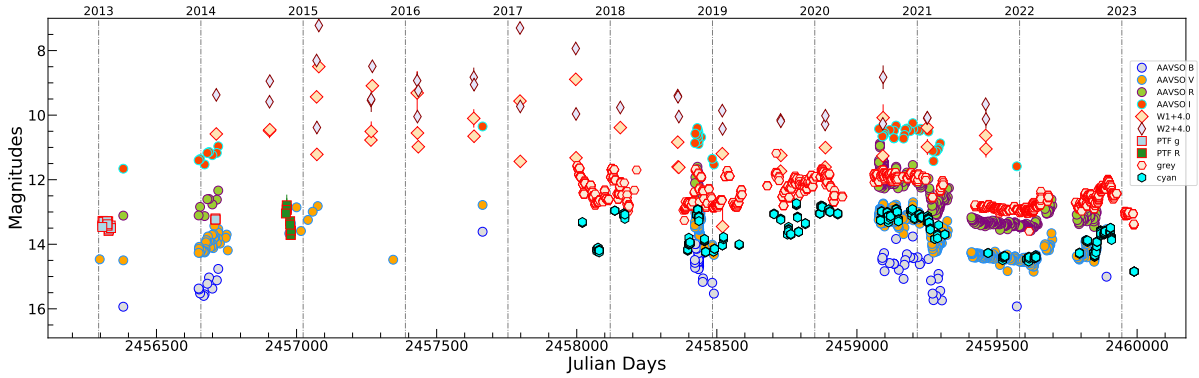

Figure 1: Light curve of XZ Tau in Johnson–Cousins B, V, R_C and I_C, ZTF zg and zr, PTF g' and R, and NEOWISE $W1$ and $W2$ bands. The AAVSO survey multi-band photometric data is labeled with AAVSO prefix whereas the Palomar survey data is prefixed with PTF. The ATLAS survey data is denoted by the cyan and orange levels respectively. The NEOWISE $W1$ and $W2$ magnitudes are scaled by 4 mag to bring forth the variations in light curve more clearly.

again, reaching 11.6 magnitude on January 06, 2018, after which it gradually faded to 13.0 magnitudes in *orange* on March 06, 2018. Between September 18, 2018 and November 01, 2018, XZ Tau brightened from 12.9 magnitudes in *orange* to 11.6 magnitudes. During the same time period, it brightened by ~ 1 magnitude in the B and V bands, reaching peak brightnesses of 13.6 and 12.5 magnitudes, respectively. The R and I bands also display similar evolution during this period, reaching peak magnitudes of 11.5 and 10.4 magnitudes, respectively. It started to decay from peak brightness reaching a minimum on January 06, 2019 with $\Delta m \simeq 1.2$, 2, 2 and 1 magnitudes in the *orange*, B, V and I bands, respectively. Another brightening event was recorded by the ATLAS survey starting from September 10, 2019 and reaching maximum brightnesses of 11.7 and 12.8 magnitudes in the *orange* and *cyan* bands, respectively on January 26, 2020. During this interval, Δm was 1 magnitude in both the *orange* and the *cyan* bands. After January 26, 2020, XZ Tau faded by approximately 0.5 magnitudes in both *orange* and *cyan* bands. The brightness of XZ Tau remained almost constant for the rest of 2020. In 2021, XZ Tau exhibited a sudden fading event with $\Delta m \simeq 1$ magnitude in the *orange*, B, V and I bands. Following this fading event, the brightness of XZ Tau started to rise, almost reaching the brightness levels of the pre-fading level. The LC of XZ Tau was stable for the rest of 2021. Starting from January 01, 2022, the R band brightness rose by ~ 0.8 magnitudes to 12.6 while the variation in ΔV and Δ*orange* were ~ 0.9 magnitudes and 0.7 magnitudes, respectively, with peak V and *orange* band magnitudes of 13.6 and 12.4, respectively. These brightness variations occurred over a period of 113 days. Another brightness variation is observed beginning from September 25, 2022, in which Δm varied by almost 0.8, 1 and 1 magnitudes in the *orange*, V and *cyan* bands respectively, after which the magnitudes returned to their pre-brightening levels of 13.4 and 14.8 in the *orange* and *cyan* bands on February 14, 2023.

The MIR LC of XZ Tau shows an overall decay in brightness from February 25, 2014

to the end of our coverage on September 03, 2021. At MIR wavelengths, XZ Tau faded by ~ 0.5 magnitudes in the $W1$ and 0.7 magnitudes in the $W2$ band. The MIR LC displays a huge scatter which can be attributed to the fact that individual NEOWISE measurements are noisy. The uncertainty in individual NEOWISE measurements can arise from a variety of factors which are highlighted on the NEOWISE website (https://wise2.ipac.caltech.edu/docs/release/neowise/expsup/sec3_2.html). The uncertainty in individual NEOWISE measurements is less than 0.05 magnitudes. Further analysis of MIR data has been done by taking the median value of the individual magnitude measurements for a given Julian day (typically three to five exposures for a given Julian day) and the error is estimated by taking the standard deviation of the magnitude variations. This has been done to estimate the error in the individual measurements as the photometric error in individual measurements are small. Previously, similar method has been employed in the case of V2493 Cyg by Ghosh et al. (2023a) to deduce its long-term brightening from the similarly noisy individual NEOWISE measurements.

The brightness variations observed in the LC can be due to fluctuations in the accretion rate or due to change in line of sight extinctions or a combination of both. We will investigate the variations in the next section based on the color evolution of XZ Tau.

3.2. Color analysis

In this section, we will investigate about the brightness variations that we observe in the LC of XZ Tau. YSOs like XZ Tau display brightness fluctuations that are driven by several factors. According to Herbst (2018), the PMS variability can be classified into three broad categories: Type-I variability which is attributed to the stellar spots modulated by the stellar rotation period having typical variability amplitude of 0.1 magnitudes; Type-II variability which is driven by accretion; Type-III variability, also known as "dippers," which occurs due to the occultation of the central PMS star by matter within the disk, that causes the observed variations. The Type-II and Type-III variability can be distinguished by their slopes of color evolution in the color-magnitude diagram (CMD) plane. The dippers follow the slope of the extinction vector, whereas Type-II sources exhibit slopes that are different from that of the extinction vector. This scheme has previously been followed by Hillenbrand et al. (2022). Figure 2 (left panel) shows the color evolution of XZ Tau during our monitoring period in V vs. $(V-R)$ CMD plane. We have also drawn an extinction vector of $A_V = 1$ magnitude to compare the slope of the color variations with that of the extinction variations. From Fig. 2 (left panel), it is evident that the slope of the color evolution of XZ Tau is distinctively different from that of the extinction vector. This implies that the probable cause of the observed variability to be driven by accretion as the dominant factor. This implies that XZ Tau is possibly displaying Type-II variability. From the left panel of Fig. 2, it also evident that there is a distinct clustering of the position of XZ Tau in the optical CMD for the time period between mid-2021 to mid-2022 which is probably due to a combination of decrease in the accretion flux and increase in extinction which resulted in the red-ward movement of XZ Tau in CMD plane.

Recent theoretical advancements in the field of episodic accretion by Liu et al. (2022) have led us to better understanding of the MIR color evolution. Their models define regions of the

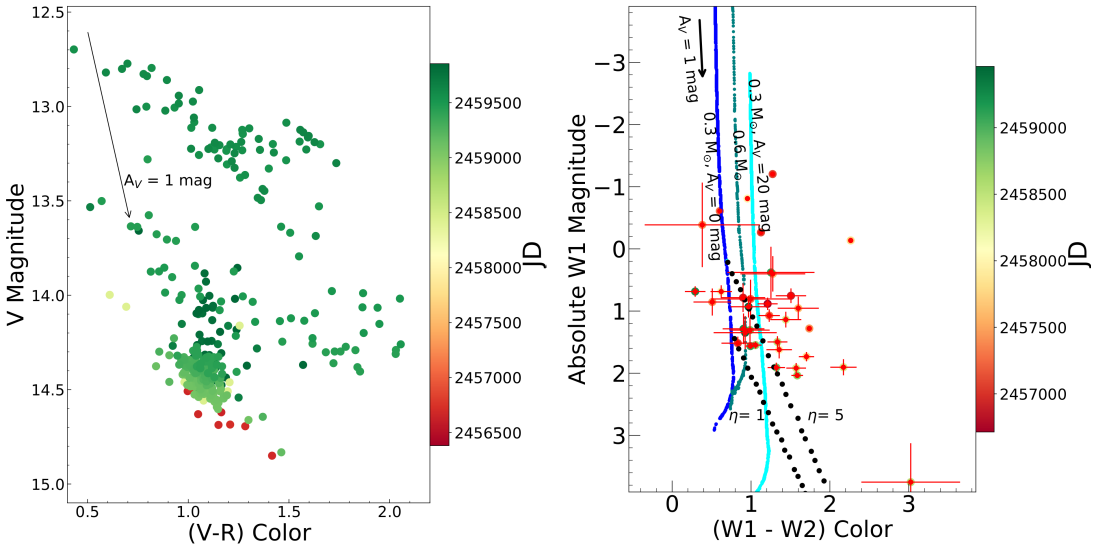

Figure 2: (*Left*) Color evolution of XZ Tau in the V vs. $(V-R)$ color-magnitude plane between 2013 and 2023. A reddening vector of $A_V = 1$ mag is drawn to show the photometric color evolution based on extinction alone. (*Right*) Evolution of XZ Tau in the $W1$ absolute magnitude vs. $W1-W2$ color plane with time. The model isomass curves obtained from Liu et al. (2022) for $0.3\,M_\odot$, $A_V = 0$ mag and $A_V = 20$ mag and for mass $0.6\,M_\odot$ is plotted to highlight the movement of XZ Tau in MIR CMD across the transition ($\eta = 1$) and sufficient dominance ($\eta = 5$) regions due to changes in accretion.

MIR CMD plane into transition ($\eta = 1$) and sufficient dominance regions ($\eta = 5$) which are based on the competitive dominance between the photospheric emission and disk emission. At low accretion rates, the stellar photospheric radiation is dominant with the contribution of the redder flux coming from disk and vice versa (Liu et al., 2022). The MIR color evolution of XZ Tau also points towards gradual decline in accretion rate resulting in migration towards the $\eta = 1$ line from the $\eta = 5$ line as evident from the right panel of Fig. 2.

3.3. Spectral features

Figure 3 shows the continuum normalized medium resolution spectra of XZ Tau obtained using TANSPEC and HFOSC respectively. The bottom panel of Fig. 3 shows the zoomed-in view of the line profiles presented here. The main spectroscopic features that are identified in the TANSPEC spectrum are the absorption features in the CO bandheads of (2–0) and (3–1) transitions, the 2.2 μm Na I and the 1.083 μm He I lines. The spectrum also exhibits emission features in hydrogen recombination lines of Brackettγ, Paschenβ, Hα and Ca II infrared triplet (IRT) lines. A detailed analysis of the line profiles has already been reported in our previous work Ghosh et al. (2023b). In summary, the observed line profiles with TANSPEC point towards the magnetospheric accretion regime in XZ Tau. The HFOSC spectrum was obtained almost two and a half years after the TANSPEC spectrum. Comparing our HFOSC spectrum with

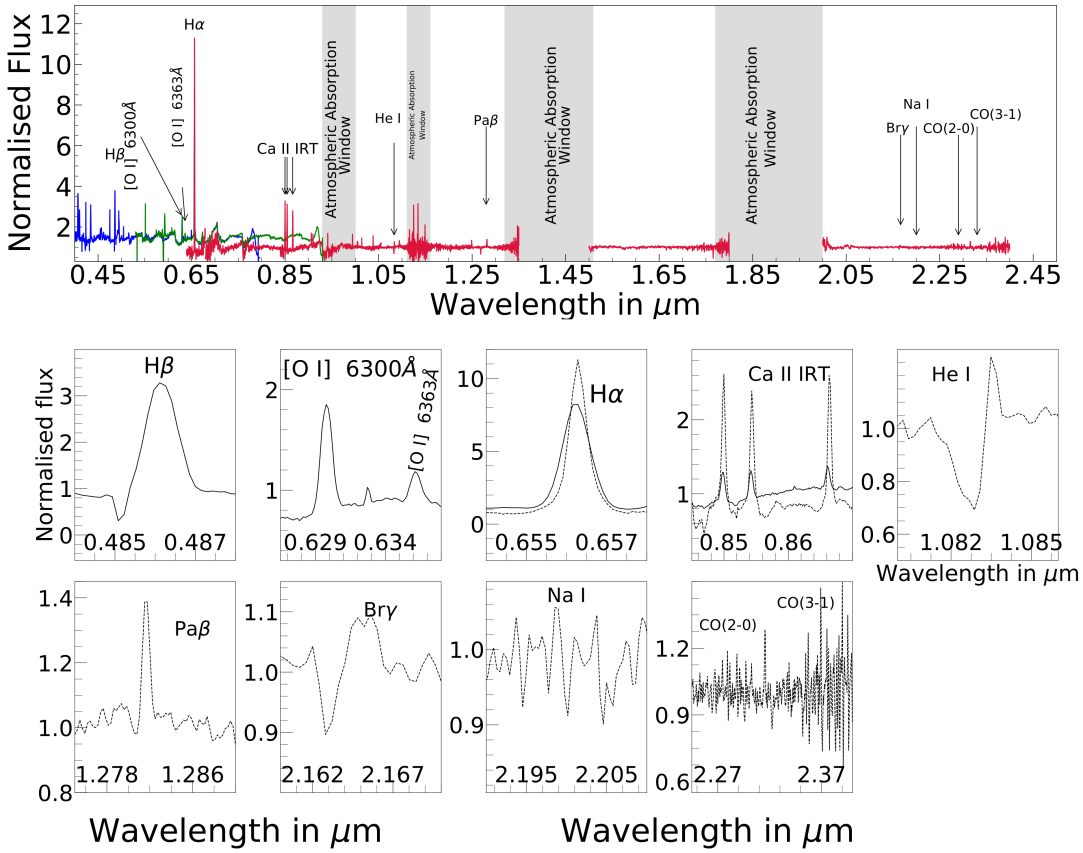

Figure 3: The top panel shows the continuum normalized spectra of XZ Tau obtained during our monitoring period using HFOSC with the 2 m HCT ($\sim$ 0.4–0.9 μm) and TANSPEC with the 3.6 m DOT ($\sim$ 0.65–2.4 μm). The HFOSC spectra were taken using the Gr. 7 and Gr. 8 grisms and are shown in blue and green, respectively; the TANSPEC spectrum is shown in red. Important spectral features of XZ Tau are marked in the spectra. The bottom panels show the zoomed-in view of the line profiles that have been used in the present study. The solid and dashed lines represent the HFOSC and TANSPEC line profiles, respectively

that of the optical part of the TANSPEC spectrum, we observe that the spectrum still exhibits the emission features in Hα and Ca II IRT, but the normalized fluxes of the spectral features are reduced in the latest spectra. This is also supported by our photometric monitoring which clearly shows that the magnitude of XZ Tau dimmed by $\sim$ 1.4 and 1.7 magnitudes, respectively in the *orange* and *cyan* bands between October 2020 and February 2023. The decrease in normalized fluxes of Hα and Ca II IRT can be likely attributed to a decrease in the accretion rate. The most interesting spectroscopic features of XZ Tau that we have observed are the P Cygni profile in Hβ and the forbidden transitions of oxygen at 6300 Å and 6363 Å. The observed P Cygni profile in Hβ line is indicative of outflowing winds from regions close to accretion as it has a similar origin than Hα (Ghosh et al., 2022). The forbidden emission lines in YSOs are believed to originate in jets and winds around the central star (Kwan, 1997). The presence of the forbidden transitions in oxygen at 6300 and 6363 Å therefore indicate outflowing jets from XZ Tau.

4. Discussion and Conclusion

We have presented here the initial results of our spectro-photometric monitoring of XZ Tau. During our monitoring period, XZ Tau exhibited multiple episodes of small scale brightening events of $\Delta m \sim 1$ magnitude in the optical regime. Such magnitude variations were not observed in the MIR regime during our monitoring period. The MIR magnitudes show an overall decline by $\sim$ 0.5 and 0.7 magnitudes respectively during our monitoring period. The optical color evolution of XZ Tau during our monitoring period can possibly be attributed to the variations in the accretion rate. In this regard, we can possibly classify the variability exhibited by XZ Tau to be of Type-II variability based on the Herbst (2018) classification scheme. We have monitored XZ Tau spectroscopically on two epochs. The emission features in the hydrogen recombination lines and the Ca II IRT lines implies that XZ Tau to be accreting via the magnetospheric accretion regime (Folha et al., 1997; Muzerolle et al., 1998). There is a decrease in the normalized flux of Hα and Ca II IRT lines between our two epochs of observations which further lends weight to our finding that the observed photometric color variations are driven by changes in the accretion rate. The HFOSC spectrum of XZ Tau displays a P Cygni profile in Hβ, indicative of outflowing winds from regions close to accretion. Forbidden lines of oxygen [O I] λ6300 and λ6363 Å have also been observed in the HFOSC spectrum of XZ Tau which indicates the presence of outflowing jets from XZ Tau. We plan to further undertake spectro-photometric observations of XZ Tau in future to understand the evolution of the accretion and outflowing jets and winds with that of the photometric color changes.

Acknowledgments

We thank the staff at the 3.6 m DOT, Devasthal (ARIES), for their co-operation during observations. It is a pleasure to thank the members of 3.6 m DOT team and IR astronomy group at TIFR for their support during TANSPEC observations. TIFR-ARIES Near Infrared Spectrometer (TANSPEC) was built in collaboration with TIFR, ARIES and MKIR, Hawaii for the DOT. We thank the staff of IAO, Hanle and CREST, Hosakote, that made these observations

possible. The facilities at IAO and CREST are operated by the Indian Institute of Astrophysics. JPN, DKO and KS acknowledge the support of the Department of Atomic Energy, Government of India, under project Identification No. RTI 4002. We acknowledge with thanks the variable star observations from the AAVSO International Database contributed by observers worldwide and used in this research. We also acknowledge the ATLAS and the NEOWISE observations that have been used in this research. We also thank the BINA organizers for offering us the opportunity to showcase our work on their platform.

Further Information

Authors' ORCID identifiers

0000-0001-7650-1870 (Arpan GHOSH)
0000-0001-5731-3057 (Saurabh SHARMA)
0000-0001-8720-5612 (Joe Philip NINAN)
0000-0001-9312-3816 (Devendra Kumar OJHA)
0000-0002-6586-936X (Aayushi VERMA)
0009-0008-8490-8601 (Tarak Chand SAHU)
0000-0002-7485-8283 (Rakesh PANDEY)
0000-0002-7434-9681 (Koshvendra SINGH)

Author contributions

The lead author is responsible for the data acquisition, data analysis and paper writing while the project and methodology has been conceived by Saurabh Sharma, D. K. Ojha and J. P. Ninan. The rest of the co-authors helped in developing the scientific interpretations that are presented in this work.

Conflicts of interest

The authors declare no conflict of interest.

References

Audard, M., Ábrahám, P., Dunham, M. M., Green, J. D., Grosso, N., Hamaguchi, K., Kastner, J. H., Kóspál, Á., Lodato, G., Romanova, M. M., Skinner, S. L., Vorobyov, E. I. and Zhu, Z. (2014) Episodic accretion in young stars. In Protostars and Planets VI, edited by Beuther, H., Klessen, R. S., Dullemond, C. P. and Henning, T., pp. 387–410. https://doi.org/10.2458/azu_uapress_9780816531240-ch017.

Bellm, E. C., Kulkarni, S. R., Graham, M. J., Dekany, R., Smith, R. M., Riddle, R., Masci, F. J., Helou, G., Prince, T. A., Adams, S. M., Barbarino, C., Barlow, T., Bauer, J., Beck,

R., Belicki, J., Biswas, R., Blagorodnova, N., Bodewits, D., Bolin, B., Brinnel, V., Brooke, T., Bue, B., Bulla, M., Burruss, R., Cenko, S. B., Chang, C.-K., Connolly, A., Coughlin, M., Cromer, J., Cunningham, V., De, K., Delacroix, A., Desai, V., Duev, D. A., Eadie, G., Farnham, T. L., Feeney, M., Feindt, U., Flynn, D., Franckowiak, A., Frederick, S., Fremling, C., Gal-Yam, A., Gezari, S., Giomi, M., Goldstein, D. A., Golkhou, V. Z., Goobar, A., Groom, S., Hacopians, E., Hale, D., Henning, J., Ho, A. Y. Q., Hover, D., Howell, J., Hung, T., Huppenkothen, D., Imel, D., Ip, W.-H., Ivezić, Ž., Jackson, E., Jones, L., Juric, M., Kasliwal, M. M., Kaspi, S., Kaye, S., Kelley, M. S. P., Kowalski, M., Kramer, E., Kupfer, T., Landry, W., Laher, R. R., Lee, C.-D., Lin, H. W., Lin, Z.-Y., Lunnan, R., Giomi, M., Mahabal, A., Mao, P., Miller, A. A., Monkewitz, S., Murphy, P., Ngeow, C.-C., Nordin, J., Nugent, P., Ofek, E., Patterson, M. T., Penprase, B., Porter, M., Rauch, L., Rebbapragada, U., Reiley, D., Rigault, M., Rodriguez, H., van Roestel, J., Rusholme, B., van Santen, J., Schulze, S., Shupe, D. L., Singer, L. P., Soumagnac, M. T., Stein, R., Surace, J., Sollerman, J., Szkody, P., Taddia, F., Terek, S., Van Sistine, A., van Velzen, S., Vestrand, W. T., Walters, R., Ward, C., Ye, Q.-Z., Yu, P.-C., Yan, L. and Zolkower, J. (2019) The Zwicky Transient Facility: System overview, performance, and first results. PASP, 131(995), 018002. https://doi.org/10.1088/1538-3873/aaecbe.

Evans, I., Neal J., Dunham, M. M., Jørgensen, J. K., Enoch, M. L., Merín, B., van Dishoeck, E. F., Alcalá, J. M., Myers, P. C., Stapelfeldt, K. R., Huard, T. L., Allen, L. E., Harvey, P. M., van Kempen, T., Blake, G. A., Koerner, D. W., Mundy, L. G., Padgett, D. L. and Sargent, A. I. (2009) The *Spitzer* c2d Legacy results: Star-formation rates and efficiencies; evolution and lifetimes. ApJ, 181(2), 321–350. https://doi.org/10.1088/0067-0049/181/2/321.

Folha, D., Emerson, J. and Calvet, N. (1997) Winds and accretion in T Tauri stars: Paschen beta line profiles. In Herbig-Haro Flows and the Birth of Stars, edited by Reipurth, B. and Bertout, C., vol. 182 of *IAUS*, pp. 272–274. https://ui.adsabs.harvard.edu/abs/1997IAUS..182P.272F.

Ghosh, A., Sharma, S., Ninan, J. P., Ojha, D. K., Bhatt, B. C., Kanodia, S., Mahadevan, S., Stefansson, G., Yadav, R. K., Gour, A. S., Pandey, R., Sinha, T., Panwar, N., Wisniewski, J. P., Cañas, C. I., Lin, A. S. J., Roy, A., Hearty, F., Ramsey, L., Robertson, P. and Schwab, C. (2022) *Gaia* 20eae: A newly discovered episodically accreting young star. ApJ, 926(1), 68. https://doi.org/10.3847/1538-4357/ac41c2.

Ghosh, A., Sharma, S., Ninan, J. P., Ojha, D. K., Bhatt, B. C., Sahu, D. K., Baug, T., Yadav, R. K., Irawati, P., Gour, A. S., Panwar, N., Pandey, R., Sinha, T. and Verma, A. (2023a) Post-outburst evolution of bona fide FU Ori-type V2493 Cygnus: A spectro-photometric monitoring. ApJ, 954(1), 82. https://doi.org/10.3847/1538-4357/ace32a.

Ghosh, S., Ninan, J. P., Ojha, D. K. and Sharma, S. (2023b) PYTANSPEC: A data reduction package for TANSPEC. JApA, 44(1), 30. https://doi.org/10.1007/s12036-023-09926-y.

Hartmann, L., Herczeg, G. and Calvet, N. (2016) Accretion onto pre-main-sequence stars. ARA&A, 54, 135–180. https://doi.org/10.1146/annurev-astro-081915-023347.

Herbst, W. (2018) The variability of young stellar objects: An update. JAVSO, 46(1), 83. https://app.aavso.org/jaavso/article/3402.

Hillenbrand, L. A., Kiker, T. J., Gee, M., Lester, O., Braunfeld, N. L., Rebull, L. M. and Kuhn, M. A. (2022) A Zwicky Transient Facility look at optical variability of young stellar objects in the North America and Pelican nebulae complex. AJ, 163(6), 263. https://doi.org/10.3847/1538-3881/ac62d8.

Kenyon, S. J., Hartmann, L. W., Strom, K. M. and Strom, S. E. (1990) An IRAS survey of the Taurus–Auriga molecular cloud. AJ, 99, 869. https://doi.org/10.1086/115380.

Kwan, J. (1997) Jets, disk winds, and warm disk coronae in classical T Tauri stars. In Herbig–Haro Flows and the Birth of Stars, edited by Reipurth, B. and Bertout, C., vol. 182 of *IAUS*, pp. 443–454. Kluwer Academic Publishers, Dordrecht (NL). https://doi.org/10.1007/978-94-011-5608-0_36.

Larson, R. B. (1969) Numerical calculations of the dynamics of collapsing proto-star. MNRAS, 145, 271. https://doi.org/10.1093/mnras/145.3.271.

Law, N. M., Kulkarni, S. R., Dekany, R. G., Ofek, E. O., Quimby, R. M., Nugent, P. E., Surace, J., Grillmair, C. C., Bloom, J. S., Kasliwal, M. M., Bildsten, L., Brown, T., Cenko, S. B., Ciardi, D., Croner, E., Djorgovski, S. G., van Eyken, J., Filippenko, A. V., Fox, D. B., Gal-Yam, A., Hale, D., Hamam, N., Helou, G., Henning, J., Howell, D. A., Jacobsen, J., Laher, R., Mattingly, S., McKenna, D., Pickles, A., Poznanski, D., Rahmer, G., Rau, A., Rosing, W., Shara, M., Smith, R., Starr, D., Sullivan, M., Velur, V., Walters, R. and Zolkower, J. (2009) The Palomar Transient Factory: System overview, performance, and first results. PASP, 121(886), 1395–1408. https://doi.org/10.1086/648598.

Liu, H., Herczeg, G. J., Johnstone, D., Contreras-Peña, C., Lee, J.-E., Yang, H., Zhou, X., Yoon, S.-Y., Lee, H.-G., Kunitomo, M. and Jose, J. (2022) Diagnosing FU Ori-like sources: The parameter space of viscously heated disks in the optical and near-infrared. ApJ, 936(2), 152. https://doi.org/10.3847/1538-4357/ac84d2.

Lorenzetti, D., Antoniucci, S., Giannini, T., Li Causi, G., Ventura, P., Arkharov, A. A., Kopatskaya, E. N., Larionov, V. M., Di Paola, A. and Nisini, B. (2012) On the nature of EXor accretion events: An infrequent manifestation of a common phenomenology? ApJ, 749(2), 188. https://doi.org/10.1088/0004-637X/749/2/188.

Lorenzetti, D., Larionov, V. M., Giannini, T., Arkharov, A. A., Antoniucci, S., Nisini, B. and Di Paola, A. (2009) Near-infrared spectroscopic monitoring of EXor variables: First results. ApJ, 693(2), 1056–1073. https://doi.org/10.1088/0004-637X/693/2/1056.

Mainzer, A. K., Bauer, J. M., Cutri, R. M., Grav, T., Masiero, J. R., Wright, E. L., Nugent, C., Stevenson, R. and Fabinsky, B. (2014) NEOWISE: A mid-infrared synoptic survey. Abstract 217.08. 223rd AAS Meeting.

Muzerolle, J., Hartmann, L. and Calvet, N. (1998) Emission-line diagnostics of T Tauri magnetospheric accretion. I. Line profile observations. AJ, 116(1), 455–468. https://doi.org/10.1086/300428.

Safron, E. J., Fischer, W. J., Megeath, S. T., Furlan, E., Stutz, A. M., Stanke, T., Billot, N., Rebull, L. M., Tobin, J. J., Ali, B., Allen, L. E., Booker, J., Watson, D. M. and Wilson, T. L. (2015) HOPS 383: an outbursting Class 0 protostar in Orion. ApJL, 800(1), L5. https://doi.org/10.1088/2041-8205/800/1/L5.

Sharma, S., Ojha, D. K., Ghosh, A., Ninan, J. P., Ghosh, S., Ghosh, S. K., Manoj, P., Naik, M. B., D'Costa, S. L. A., Krishna Reddy, B., Nanjappa, N., Pandey, R., Sinha, T., Panwar, N., Antony, S., Kaur, H., Sahu, S., Bangia, T., Poojary, S. S., Jadhav, R. B., Bhagat, S. B., Meshram, G. S., Shah, H., Rayner, J. T., Toomey, D. W., Sandimani and Pradeep R. (2022) TANSPEC: TIFR–ARIES near-infrared spectrometer. PASP, 134(1038), 085002. https://doi.org/10.1088/1538-3873/ac81eb.

Shu, F. H. (1977) Self-similar collapse of isothermal spheres and star formation. ApJ, 214, 488–497. https://doi.org/10.1086/155274.

Terebey, S., Shu, F. H. and Cassen, P. (1984) The collapse of the cores of slowly rotating isothermal clouds. ApJ, 286, 529–551. https://doi.org/10.1086/162628.

Tonry, J. L., Denneau, L., Heinze, A. N., Stalder, B., Smith, K. W., Smartt, S. J., Stubbs, C. W., Weiland, H. J. and Rest, A. (2018) ATLAS: A high-cadence all-sky survey system. PASP, 130(988), 064505. https://doi.org/10.1088/1538-3873/aabadf.